Direct Observation of Velocity-Tuned Multiphoton Processes in the Laser Cavity

J. Reid* and Takeshi Oka
Herzberg Institute of Astrophysics, National Research Council of Canada, Ottawa, Ontario, Canada

(Received 26 October 1976)

The transmission characteristics of molecules subjected to an intense standing-wave laser radiation are monitored by a probe laser. In addition to the usual Bennett holes, we observe several saturated absorption and emission features caused by velocity-tuned multiphoton processes. These direct experimental observations confirm the theoretical predictions of Haroche and Hartmann.

Since the development of the laser there has been a great deal of interest in saturated-absorption phenomena. The initial work by authors such as Bennett[1] and Lamb[2] dealt experimentally and theoretically with two-level systems subjected to intense standing-wave radiation. This work led to the concept of burning Bennett holes in the Maxwellian profile of a gaseous absorber, and the occurrence of Lamb dips when these holes are tuned through the resonance frequency. Recent theoretical papers[3-7] considered these processes in greater detail, and carried out calculations to higher orders of perturbation. In particular, Haroche and Hartmann[3] considered a two-level system subjected to irradiation by a strong pump field and a weak probe field propagating in opposite directions. They predicted that, because of higher-order multiphoton processes, the transmitted probe radiation will show sharp nonresonant absorption and emission features which had not been considered in the normal hole-burning model. We report the first direct experimental observation of these features. This observation confirms the existence of the predicted multiphoton processes and suggests that such processes play an important role in other multiphoton experiments and in the theory of lasers.

The experimental arrangement is similar to the usual in-cavity–absorption Lamb-dip apparatus. A cell containing a low-pressure absorbing gas is placed in a CO_2 laser cavity; the gas (CH_3F) and the laser line are selected such that the laser frequency ω_l can be tuned within the Doppler profile of a strong molecular absorption centered at ω_0. In a conventional Lamb-dip experiment, the existence of hole burning is observed by tuning ω_l through ω_0 and monitoring the laser output power. However, we wish to detect nonresonant-absorption features and hence ω_l is held fixed and off center. The interaction of the molecules with the intense pump-laser radiation is then monitored using a second probe laser whose frequency ω is swept over the Doppler profile. This arrangement is slightly different from that considered by Haroche and Hartmann[3] in that the pump radiation is propagating in both directions.

Figure 1 is a schematic diagram of the apparatus. The absorption cell is 50-cm long and sealed with two ZnSe Brewster-angle windows. To min-

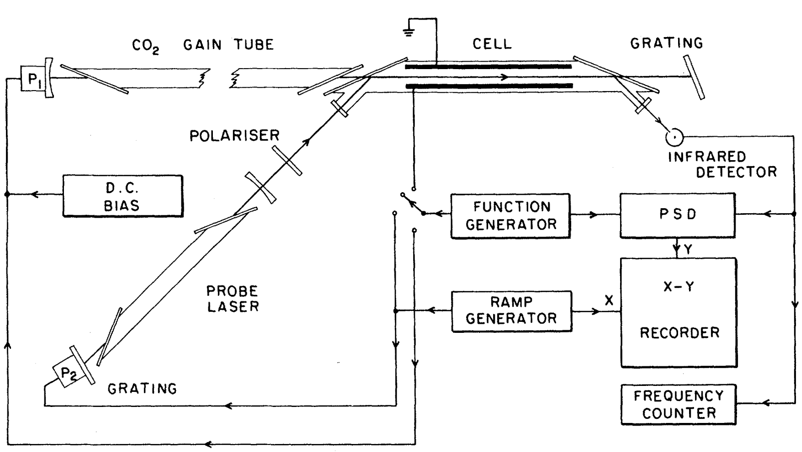

FIG. 1. Schematic diagram of the apparatus.

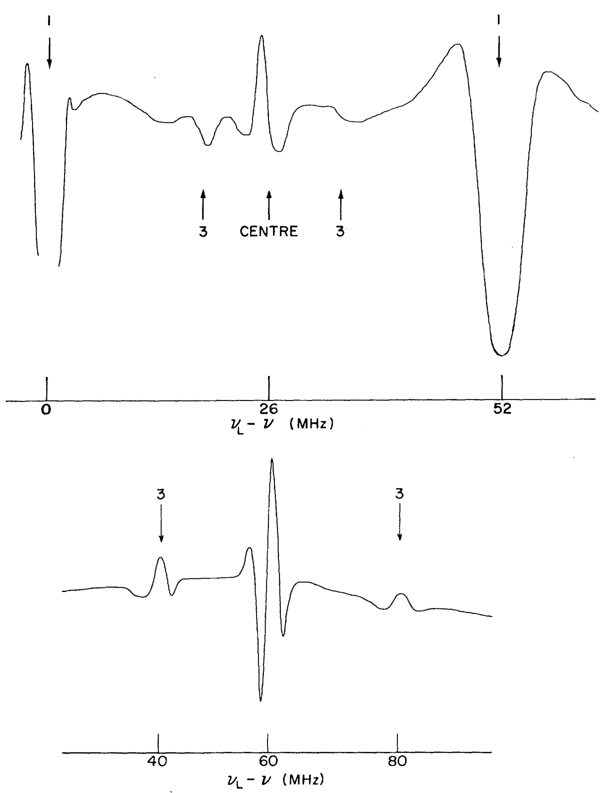

FIG. 2. Examples of the observed spectrum. Features "1," "center," and "3" correspond to the Bennett holes, the two-photon (Rayleigh) process, and the three-photon (Raman) process, respectively.

imize any interaction between the pump and probe lasers, their beams were arranged to be orthogonally polarized in the cell. This was achieved by reflecting the probe beam from the ZnSe windows of the cell. This is a convenient method of ensuring that only the component of the probe beam which is polarized perpendicular to the pump radiation will be reflected into the cell. A rotatable polarizer was placed in the probe beam, and used to control the probe intensity in the cell. The probe radiation was generated by a short, low-powered laser and was frequency-swept using the piezoelectric translator, P_2. We carried out experiments on two different absorber/laser coincidences. These were the $\nu_2{}^qR(4, 3)$ line of $^{13}CH_3F$ which lies 25.8 MHz below the CO_2 $P(32)$ 9.4-μm line, and the $\nu_2{}^qQ(12, 2)$ line of $^{12}CH_3F$ which lies 44.2 MHz above the $P(20)$ 9.4-μm line.[8] The frequency offset $\Delta\omega = \omega_0 - \omega_l$ was varied by applying a voltage to the piezoelectric translator P_1. The pump-laser intensity in the cell was ~ 100 W/cm^2, while the probe intensity was less than 0.1 W/cm^2. The probe beam was detected by a Pb-Sn-Te detector and the signal was processed with a phase-sensitive detector. Three different types of modulation was used to increase the sensitivity of detection; Stark modulation of the gas and frequency modulation of either the pump or probe lasers. While Stark modulation gave the best sensitivity of detection and symmetry of observed signals, the existence of such effects as transient nutation and level crossing[9] sometimes complicated the line shape. Frequency modulation of the probe laser was particularly helpful in interpreting line shapes. The frequency offset of the two lasers was monitored by measuring their beat frequency with a frequency counter.

Examples of the observed signals are shown in Fig. 2. To obtain the results shown in the upper trace, the pump laser was tuned to the center of the CO_2 $P(32)$ line (that is, 25.8 MHz above the center of the absorption profile of $^{13}CH_3F$) and the probe laser was swept over about 60 MHz. The trace was recorded using 15-kHz Stark modulation, with the modulation field perpendicular to the pump-laser field. The large, broad signals marked 1 are the saturation-broadened Bennett holes corresponding to molecules with axial velocities which satisfy the single-photon resonance condition

$$\omega_0 = \omega_\pm \equiv (1 \pm v/c)\omega_l. \tag{1}$$

The widths of the Bennett holes are of the order of $\langle 1 | \mu E | 2 \rangle / h$ (~ 7 MHz in this case).

In addition to this well-known phenomenon, we saw the sharp multiphoton features predicted by Haroche and Hartmann at the central portion of the spectrum. The sharp feature at the center is caused by a two-level, two-photon process which Haroche and Hartmann called the Rayleigh process. The velocity matching for this process is

$$\omega_\pm - \omega_\mp = \pm 2v\omega_l/c = 0, \tag{2}$$

that is, $v = 0$. This signal is not caused by population changes as are the other signals, but by coherent driving of the molecules by the pump radiation. As predicted by Haroche and Hartmann, the signal was observed to be dispersive in shape in contrast to the other signals. The sharp features marked 3 are due to a three-photon process which Haroche and Hartmann called the Raman process. The velocity matching for this process is

$$\omega_0 = \omega_\pm - \omega_\mp + \omega_\pm = (1 \pm 3v/c)\omega_l, \tag{3}$$

and therefore the hole burning occurs at an axial velocity which is one third of that for the single-photon Bennett hole. Our measurement of the beat frequency of the pump and probe lasers confirmed this. The effect of this three-photon process has been already noted indirectly in the infrared–radio-frequency two-photon Lamb-dip spectrum.[10] Such processes were called *velocity-tuned multiphoton processes*. A simple third-order time-dependent perturbation treatment gives the transition moment of the velocity-tuned three-photon process to be[7]

$$M_3 = 9\langle 1|\mu\cdot E|2\rangle^3/16h^3(\nu_l-\nu)^2 \qquad (4)$$

in units of frequency. For the present experimental condition ($\langle 1|\mu\cdot E|2\rangle \sim 7$ MHz, $\Delta\nu \sim 30$ MHz), M_3 is about 200 kHz and sufficiently high so that the three-photon transition is saturated for a low-pressure gas (the pressure broadening of CH_3F at 10 mTorr is about 200 kHz).

The lower trace of Fig. 2 demonstrates in more detail the central portion of the spectrum. To obtain this spectrum, we set the pump laser 60 MHz above the center of molecular absorption. Thus, the center feature and the three-photon features are better separated than in the upper trace. This picture shows rather clearly the difference in line shape between the center and the three-photon features. This trace was also taken using Stark modulation with an electric field parallel to the pump-laser field.

While our observation confirmed all the predicted features of the theory of Haroche and Hartmann, we observed some extra features because we used standing-wave pump radiation. We saw single-photon and three-photon holes burned on both sides of the center, and also saw asymmetries introduced into the hole-burning processes because the probe radiation is propagating only in one direction. Our observations are best explained by using a density-matrix theory similar to the one developed by Shimizu for two-photon Lamb dips.[5,7] The response of an ensemble of molecules with an axial velocity v is described by a density-matrix equation

$$\dot{\rho} = -i[H,\rho]/\hbar - \gamma(\rho - \rho^{(0)}), \qquad (5)$$

where the Hamiltonian $H = H_3 - \mu\cdot\epsilon$ includes both the standing-wave pump field $E_\pm$ and the probe field E

$$2\epsilon = E_+\exp[i(\omega_l - kv)t] + E_-\exp[i(\omega_l + kv)t] + E\exp[i(\omega + kv)t] + \text{c.c.} \qquad (6)$$

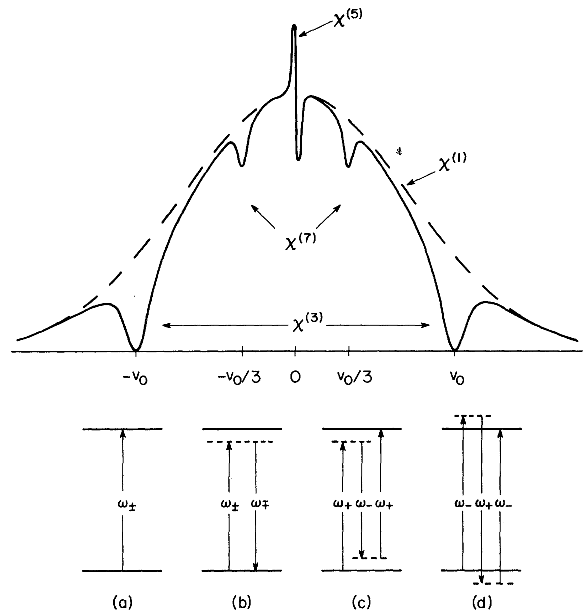

FIG. 3. Schematic spectrum predicted by the perturbation theory and energy diagrams. $\chi^{(1)}$ is the Voigt profile for the probe radiation. $\chi^{(3)}$ denotes Bennett holes due to single-photon process (a). $\chi^{(5)}$ is the center feature due to two-photon process (b). $\chi^{(7)}$ is due to velocity-tuned three-photon processes (c) and (d). The asymmetry term is omitted for clarity.

Equation (5) is transformed to equations of motion for the components of the density matrix by using the standard procedure of the rotating-wave approximation.[11] The resulting equation is solved by iteration. The bulk susceptibility of the gas for the probe radiation is then obtained by considering the component of the total polarization $\mu\rho_{12}$ which has the same time variation as the probe electric field, and integrating it over the Maxwellian velocity distribution.[5,7] The various features observed in our work appear in different orders in this calculation. The results of the theoretical calculation are shown schematically in Fig. 3.

The first-order susceptibility $\chi^{(1)}$ gives the well-known Voigt absorption profile. The Bennett holes monitored with the probe radiation appear in the third-order term $\chi_\pm^{(3)}$. The asymmetry of the holes, which is of dispersive shape, also appears in the third-order $\chi_d^{(3)}$. Then the higher-order susceptibility terms give the effect of velocity-tuned multiphoton processes. The center feature which corresponds to the two-photon (Rayleigh) process appear in the fifth-order term $\chi_\pm^{(5)}$ and the three-photon (Raman) process in the seventh-order $\chi_\pm^{(7)}$. The energy diagrams for these processes are also given in Fig. 3. The single-photon process shown in Fig. 3(a) gives $\chi^{(3)}$, the two-photon process in Fig. 3(b) gives $\chi^{(5)}$ and the three-photon processes in Fig. 3(c) and 3(d) gives $\chi^{(7)}$. Note Haroche and Hartmann's three-photon diagram is corrected here. The fact that the polarization of the probe radiation is perpendicular to that of the pump radiation introduces some complexities. A more detailed description of the theory and experiment will be published elsewhere.

In summary, our observation clearly demonstrates the existence of velocity-tuned multiphoton processes in the laser cavity. Such multiphoton processes have implications in various areas of laser physics: (a) In the theory of the laser the perturbation treatment normally extends only up to the third order.[11] Many "nonresonant" molecules which are not considered in such theories may contribute to the laser power through velocity-tuned multiphoton processes. (b) For many multiphoton experiments, the use of a standing wave will increase the efficiency not only through a more intense field but also through the velocity-tuned multiphoton process. (c) As pointed out by Stenholm[6] a velocity-tuned $(2l+1)$-photon process has a momentum transfer of $2l+1$ photons in a single step. This can be used for efficient deflection of atomic or molecular beams.

We wish to thank S. Haroche and S. Stenholm for helpful discussions and E. Arimondo, P. Glorieux, and A. R. W. McKellar for critical reading of the paper.

[1]W. R. Bennett, Jr., Phys. Rev. 126, 580 (1962).

[2]W. E. Lamb, Jr., Phys. Rev. 134, A1429 (1964).

[3]S. Haroche and F. Hartmann, Phys. Rev. A 6, 1280 (1972).

[4]J. H. Shirley, Phys. Rev. A 8, 347 (1973).

[5]F. Shimizu, Phys. Rev. A 10, 950 (1974).

[6]S. Stenholm, J. Phys. B 7, 1235 (1974).

[7]T. Oka, in Proceedings of the Summer School of Theoretical Physics, Les Houches, France, 1975 (to be published).

[8]S. M. Freund, G. Duxbury, M. Römheld, J. T. Tiedje, and T. Oka, J. Mol. Spectrosc. 52, 38 (1974).

[9]P. R. Berman, J. M. Levy, and R. G. Brewer, Phys. Rev. A 11, 1668 (1975).

[10]S. M. Freund, M. Römheld, and T. Oka, Phys. Rev. Lett. 35, 1497 (1975).

[11]M. Sargent, III, M. O. Scully, and W. E. Lamb, Jr., *Laser Physics* (Addison-Wesley, Reading, Mass., 1974).

High-Pressure Flux-Conserving Tokamak Equilibria

J. F. Clarke
Oak Ridge National Laboratory, Oak Ridge, Tennessee 37830

and

D. J. Sigmar
Massachusetts Institute of Technology, Cambridge, Massachusetts 02139
(Received 26 July 1976)

An analytic theory is developed to calculate poloidal beta β_I and the diamagnetic parameter μ_I for axisymmetric toroidal magnetohydrodynamic equilibria confining high-pressure plasmas $[\beta \sim O(a/R)]$ under the constraint of flux conservation. To satisfy the equilibrium equations, the plasma current increases with pressure as $p^{1/3}$. Previously calculated equilibrium limits on poloidal β are avoided.

Successful auxiliary heating of thermonuclear plasmas requires a characteristic heating time τ_h shorter than the energy containment time τ_E. Using neutral-particle injection, tokamak experiments with $\tau_A < \tau_h \leq \tau_E$, where τ_A is the Alfvén time, have been conducted (ORMAK), and future devices (PLT, ORMAK Upgrade, TFTR) will satisfy this criterion. Experimental evidence so far (ATC, Tuman) indicates $\tau_E < \tau_S$, where τ_S is the magnetic skin penetration time. The resulting condition $\tau_h < \tau_S$ necessitates the study of a series of neighboring magnetohydrodynamic (MHD) equilibria under the constraint of flux conservation.

We will assume, consistent with experiment, that on the time scale of interest both the poloidal flux $2\pi\psi$ and toroidal flux φ are conserved. Since the safety factor q is given by $q(\psi) = (2\pi)^{-1} d\varphi/d\psi$,